Performance Analysis of Blind Adaptive MOE Multiuser Receivers Using Inverse QRD-RLS Algorithm

Ayman Elnashar, Said Elnoubi, and Hamdi A. El-Mikati, *Senior Member, IEEE*

***Abstract*—The inverse QR (IQRD) recursive least-squares (RLS) algorithm (IQRD-RLS) is very popular because it has good numerical stability and can be mapped onto COordinate Rotation DIgital Computer (CORDIC) processor-based systolic arrays, which are suitable for very large-scale integrated circuits (VLSI) architecture and real-time applications. In this paper, the blind optimal minimum output energy (MOE) detector which is developed for multiuser detection (MUD) in direct-sequence code-division multiple-access (DS-CDMA) systems is implemented using the linearly constrained IQRD-RLS algorithm. Specifically, the max/min approach is combined with subspace tracking for producing the optimal MOE multiuser detector. A new fast subspace tracking algorithm based on Lagrange multiplier methodology and the IQRD-RLS algorithm is developed. A comparative analysis among the recently emerged channel-estimation techniques is conducted using the IQRD-RLS algorithm. The corresponding robust MOE receivers at low SNR are implemented using the IQRD method, and their performances are assessed in terms of SINR, BER, and computational complexity. A robust multiuser receiver is developed by adding a quadratic inequality constraint to the optimal max/min MOE detector. The feasibility of systolic array implementation of the IQRD-based optimal MOE detector is explored. Several simulation experiments are conducted in a severe near–far environment to analyze the IQRD-based receivers and the subspace tracking algorithms.**

***Index Terms*—Constrained optimization, direct-sequence code-division multiple-access (DS-CDMA) system, inverse QR-decomposition, minimum output energy (MOE) detection, multiuser detection (MUD), subspace tracking, systolic arrays, wireless communications.**

I. Introduction

A LINEAR RECEIVER for direct-sequence code-division multiple-access (DS-CDMA) systems can be designed by minimizing an inverse filtering criterion. Appropriate constraints are utilized to avoid the trivial all-zero solution. A well-known cost function for the constrained optimization problem is the variance (i.e., power) of the receiver output. A minimum output energy (MOE) detector is developed in [1] for multiuser detection (MUD) based on the constrained optimization approach. In an additive white Gaussian noise (AWGN) environment with no multipath, this detector provides a blind solution with minimum mean-square error (MMSE) performance. Unfortunately, this approach undergoes severe performance degradation in the presence of signal mismatch, inter-chip interference (ICI), and multipath propagation [2]. An improved constrained optimization approach to handle multipath fading is presented in [2], where only the main multipath component is used and other delayed components are forced to zero. This approach is not the optimal solution; although it can handle the multipath case, but it did not maximize the signal-to-interference-plus-noise ratio (SINR). An optimal solution is proposed in [3] where the channel vector is obtained by a max/min approach. The theoretical performance of this method tends to be close to the optimal nonblind MMSE receiver at high signal-to-noise ratio (SNR) in the presence of multipath fading. Adaptive implementation algorithms for this method are presented in [4]. This method requires eigenvalue decomposition which requires additional complexity. Additionally, the max/min approach is notorious to exhibits some performance degradation at low SNR. Robust constrained optimization approaches are developed in [5] and [6] by using a fixed set of linear constraints that do not need to be optimized, plus a quadratic inequality constraint (QIC) on the weight vector norm. These techniques provide robust DS-CDMA detectors with low computational complexity. The QIC is employed to handle random perturbations and mismatch errors. In addition, the QIC can overcome noise enhancement at low SNR [6]. These approaches are built on the generalized sidelobe canceller (GSC) structure by imposing the QIC on the adaptive portion of the weight vector of the GSC structure. Unfortunately, these approaches depend on equal-gain combining for multipath components and hence the channel vector is not optimized.

Improved constrained MOE detectors for handling the noise enhancement at low SNR case are introduced in [7] and [8] which require minor eigenvector and corresponding eigenvalue estimation for a new cost function plus, respectively, the maximum and minimum eigenvalue of the data covariance matrix. In these approaches, the contribution of the noise is partially subtracted from the cost function [7] or completely eliminated if its power can be estimated [8]. If noise power is not perfectly known as in practical or in severe fading channels, subtraction is performed in an *ad hoc* manner by properly choosing a close

Manuscript received December 12, 2005; revised March 10, 2007. This paper was recommended by Associate Editor V. E. De Brunner.

A. Elnashar was with the Department of Mobile Network Development (MND), Etihad Etisalat (mobily), Riyadh 11423, Saudi Arabia. He is now with Technology Development Department, Emirates Integrated Telecommunications Company PJSC (du), Dubai 502666, U.A.E. (e-mail: anashar@gmail.com).

S. M. Elnoubi is with the Department of Electrical Engineering, Alexandria University, Alexandria 21544, Egypt (e-mail: selnoubi@hotmail.com).

H. A. El-Mikati is with the Department of Electronic Engineering, Mansoura University, Mansoura 35516, Egypt (e-mail: h.elmikati@ieee.org).

Digital Object Identifier 10.1109/TCSI.2007.913611

1549-8328/$25.00 © 2008 IEEE

candidate from the noise estimate [8]. Regrettably, the performance of these approaches is degraded due to the covariance matrix estimation errors.

It is shown in [3] that the channel estimation error is inversely proportional to the input SNR. Motivated by this result, Xu *et al.* [9] proposed a Power of $\boldsymbol{R_{xx}}$ (POR) receiver by boosting the power of data covariance matrix $\boldsymbol{R_{xx}}$ in the MOE cost function to a positive integer m in order to virtually amplify the SNR from estimation perspective. It is shown in [9] that the proposed MMSE receiver built on the estimated channel parameters when $m \geq 2$ asymptotically converges to the optimal MMSE receiver in terms of output SINR, thus eliminating the penalty in the MOE detector. Unfortunately, the POR method needs high computational burden due to boosting the power of data covariance matrix.

Most of the adaptive implementations developed in the literature [4]–[9] were based on the well-known recursive least-squares (RLS) algorithm. In the conventional RLS algorithm, the calculation of the Kalman gain requires matrix inversion of the covariance matrix of the received signal. If the data covariance matrix is ill-conditioned or, in the worst case, has rank less than the number of the weight vector elements, the conventional RLS algorithm will rapidly become impossible. Moreover, it cannot be implemented generally via efficient hardware architectures [10]. Furthermore, finite precision implementations of the RLS filters have sometimes been observed to be numerically unstable [11]. A distinguished approach for overcoming these shortcomings is the rotation-based QR-RLS algorithm. The QR decomposition transforms the original RLS problem into a problem that uses only transformed data values by *Cholesky* factorization of the original least-squares data covariance matrix [12]. The QRD-RLS algorithm, which is also referred as the Givens rotations or CORDIC-based RLS algorithm, is the most promising RLS algorithm because it possesses desirable properties for very large-scale integrated circuits (VLSI) implementations such as regularity and can be mapped on CORDIC arithmetic-based processors [13]. CORDIC is a class of shift-add algorithms for rotating vectors in a plane. In a nutshell, the CORDIC rotator performs a rotation using a series of specific incremental rotation angles selected so that each is performed by a shift-and-add operation. Rotation of unit vectors engenders a way to accurately compute trig functions, as well as a mechanism for computing the magnitude and phase angle of an input vector. Furthermore, the QRD-RLS algorithm exhibits a high degree of parallelism and can be mapped to triangular systolic arrays for efficient parallel implementation.

In [12], Poor and Wang investigated the use of the QRD-RLS algorithm for MUD in the context of DS-CDMA systems. Unfortunately, the QRD-RLS algorithm suffers from a major drawback, namely, back-substitution, which is a costly operation to be performed in array structure [10]. In [11], Alexander and Ghirnikar proposed a new computationally efficient algorithm for RLS filtering, which is based upon an IQRD algorithm. In the IQRD updating method, the least-squares weight vector can be calculated without back-substitution. Furthermore, the IQRD method employs orthogonal rotation operations to recursively update the filter weights and thus preserves the inherent stability properties of QR approaches to RLS filters. The IQRD-RLS algorithm is exploited in beamforming applications in [10] and [13]–[15] and deployed for MUD in [16]–[21].

In this paper, a linearly constrained IQRD-RLS algorithm with multiple constraints is developed and implemented for the MUD in DS-CDMA systems. The contributions of this paper is threefold. The first contribution is the implementation of the optimal MOE detector using the IQRD-RLS algorithm. The adopted optimal MOE detector is based on the combination of the max/min approach with a new fast subspace tracking algorithm for tracking channel vector (see also [15]–[17]). Optimization of the constrained vector by the min/max approach was introduced in [3], but in this paper the constrained vector is obtained using the IQRD-based subspace tracking algorithm. In addition, an experimental analysis is carried out on the recently proposed subspace tracking techniques when employed for max/min channel vector tracking. The second contribution of this study is the development of adaptive implementations of the recently proposed robust MOE receivers using the IQRD-RLS algorithm. In addition, a robust MOE detector is developed by adding a QIC on the weight vector norm of the first proposed algorithm to overcome noise enhancement at low SNR. A simple direct-form solution is adopted for the quadratically constraint detector with a variable loading (VL) technique is employed to satisfy the QIC. The IQRD-RLS algorithm acts as a core to the preceding receiver which facilitates real-time implementation through systolic arrays. Furthermore, a comparative analysis among the robust MOE receivers at low SNR is conducted in terms of SINR, bit error rate (BER), and computational complexity. The third contribution is the development of a systolic array implementation of the optimal IQRD-based MOE detector.

The remainder of this paper is organized as follows. In Section II, the DS-CDMA system model is formulated. The linear detection, MOE detector, and the IQRD-RLS algorithm are outlined in Section III. The design of the optimal MOE detector based on the IQRD-RLS algorithm is covered in Section IV. In Section V, the recently emerged robust MOE detectors at low SNR are summarized and implemented using the IQRD-RLS algorithm. Systolic array implementation of the optimal MOE detector using the IQRD-RLS algorithm is demonstrated in Section VI. Computer experiments and complexity analysis are provided in Section VII. Conclusions and points for future work are provided in Section VIII.

The following notations are adopted throughout the paper. Lower case letters are used for scalars, lower case bold letters are for vectors, and capital bold letters are for matrices. The vectors $\mathbf{0}_N$ and $\mathbf{1}_N$ and the matrix $\boldsymbol{I}_N$ signify, respectively, the $N \times 1$ null vector, the $N \times 1$ all-one vector, and the $N \times N$ identity matrix. Further, $(.)^*, (.)^T, (.)^H, (.)^{-H}, (.)^{-1}, \|.\|$ denote complex conjugate, transpose, Hermitian, inverse Hermitian, inverse, and magnitude, respectively. Also, $\boldsymbol{v}_i$, $\boldsymbol{\Pi}_{i,j}$, $\mathrm{Re}\{\ \}$, and $E\{\ \}$ represent, respectively, the ith component of the vector $\boldsymbol{v}$, the i,j component of the matrix $\boldsymbol{\Pi}$, the real part, and the expectation operation. Finally, $\nabla_{\boldsymbol{g}}\boldsymbol{\Psi}(n)$ stands for the gradient of $\boldsymbol{\Psi}(n)$ with respect to the real and imaginary parts of $\boldsymbol{g}^H(n)$ (sometimes termed the conjugate derivative).

II. System Model

In the DS-CDMA system, K mobile users transmit simultaneously to the base station, where each user's symbols are assumed binary phase-shift keying (BPSK) with arbitrary power and timing. Each user's symbol is multiplied by a spreading code $\boldsymbol{c}_j = [c_j(0)\cdots c_j(L-1)]^T$ of length L, where chip period $T_c = T/L$ and T is the symbol period. All users are assumed to use the same chip pulse-shaping filter, which is assumed to be time limited to $[0, T_c)$. Each user's signal is assumed to pass through a finite-impulse-response (FIR) channel including any attenuation, multipath, asynchronism, pulse-shaping filter, and front-end receiver filter. The aggregate channel noise is assumed to be zero mean Gaussian and independent from source symbols and denoted by $\boldsymbol{w}(n)$ with variance σ_w^2. The received signal is the superposition of all transmitted signals plus noise and is sampled at chip rate. Therefore, the sampled received signal $\boldsymbol{x}(n)$ is given by [3]–[6]

$$\boldsymbol{x}(n) = \sum_{j=1}^{K} \boldsymbol{u}_j(n) + \boldsymbol{w}(n) \tag{1}$$

where $\boldsymbol{u}_j(n)$ is the j^{th} user's contribution to the received signal and can be written as

$$\boldsymbol{u}_j(n) = \sum_{l=-\infty}^{\infty} \boldsymbol{s}_j(l).\boldsymbol{h}_j(n - lL - \tau_j) \tag{2}$$

where τ_j and $\boldsymbol{s}_j(n)$ represent user delay and transmitted data bits of user j, respectively.

Each user information bearing sequence $\boldsymbol{s}_j(n)$ is assumed, zero mean, i.i.d, and independent of other users. The vector $\boldsymbol{h}_j(n)$ stands for the effective signature waveform of user j, and it is the spreading sequence transmitted through channel characterized by impulse response $\boldsymbol{g}_j(t)$. Therefore, the effective signature waveform of user j is the convolution of the user code with the multipath channel and can be modeled as follows:

$$\boldsymbol{h}_j(n) = \sum_{m=-\infty}^{\infty} \boldsymbol{c}_j(m).\boldsymbol{g}_j(n-m). \tag{3}$$

Each user's signal is assumed to pass through a channel with length N_g and denoted by $\boldsymbol{g}_j(n)$, which includes any attenuation, multipath, asynchronism, pulse shaping filter, and front-end receiver filter.

Let σ_j denote the amplitude of the jth user's signal, M_j be the number of multipath components, $\alpha_{j,m}$ be the amplitude of the user's signal scattered in mth path, and $\gamma_{j,m}$ be the time delay of this path. Therefore, the combined multipath channel-pulse-shaping impulse response of the jth user (i.e., $\boldsymbol{g}_j(t)$) can be expressed as [3]–[6]

$$\boldsymbol{g}_j(t) = \sigma_j \sum_{m=0}^{M_j} \alpha_{j,m}\varphi_j(t - \gamma_{j,m}) \tag{4}$$

where $\varphi_j(t)$ is the original chip waveform, which includes the effect of the transmit and receive filter. The multipath delay spread $\gamma_{j,m}$ is chosen in this paper to be a random integer between the first and eighth chip (implying T_c and $8T_c$, respectively) and the maximum channel length N_g is limited to ten chips. This represents a practical CDMA multipath delay spread with an elliptical channel model to describe the multipath propagation condition. For example, the maximum delay spread N_gT_c will be $\approx 8\ \mu$s for the CDMA2000 system, whereas $T_c = 0.813\ \mu$s and the channel delay spread will be $\approx 3\ \mu$s for WCDMA whereas $T_c = 0.260\ \mu$s [22], [23]. Furthermore, the conducted simulations in this paper are based on Gold codes with 31 chips length. Therefore, the maximum delay spread adopted in this paper is approximately one third the code length. As a result, for the UMTS system with long codes (i.e., 256 chips), a delay spread of order 20 μs can be exemplified by the proposed system. It is noteworthy to highlight that the 3G Partnership Project (3GPP) specifies a channel with length up to 20 μs. In another example, for a TD-SCDMA system with maximum code length equaling 16 chips, the maximum multipath delay spread is five chips, which means 3.125 μs, where $T_c = 0.625\ \mu$s. According to the Gold codes with 31 chips adopted in this paper, the maximum delay of the TD-SCDMA system is almost equal to the maximum delay spread adopted in this paper.

Without loss of generality, we will assume that the user number one is the user of interest, and it is used as the timing reference ($\tau_1 = 0$). A chip-rate linear receiver can be designed by collecting N_f samples from the received signal vector, which is at least as long as the signature waveform plus the delay spread N_g. The received data vector for each symbol is collected into $N_f \times 1$ vector and can be reformulated as follows [3]:

$$\boldsymbol{x}(n) = \boldsymbol{h}_1\boldsymbol{s}_1(n) + \boldsymbol{H}_i\boldsymbol{s}_i(n) + \boldsymbol{w}(n) \tag{5}$$

where $\boldsymbol{s}_i(n)$ is the interference vector with regard to $\boldsymbol{s}_1(n)$ including intersymbol interference (ISI) and multiple access interference (MAI) and $\boldsymbol{H}_i$ is the effective signature matrix of both MAI and ISI with columns corresponding to symbols in $\boldsymbol{s}_i(n)$. The effective signature waveform of the required user $\boldsymbol{h}_1$ can be represented in a matrix form, which is beneficial in developing code-constrained receivers, as follows [23]:

$$\boldsymbol{h}_1 = \boldsymbol{C}_1.\boldsymbol{g}_1 \tag{6}$$

where

$$\boldsymbol{C}_1 = \begin{bmatrix} \boldsymbol{c}_1(L-Ng) & \cdots & \boldsymbol{c}_1(L-1) \\ & \ddots & \\ \boldsymbol{c}_1(0) & & \\ & \ddots & \boldsymbol{c}_1(0) \\ 0 & & 0 \end{bmatrix}_{N_f \times N_g}$$

$$\boldsymbol{g}_1 = \begin{bmatrix} g_1(N_g-1) \\ \vdots \\ g_1(0) \end{bmatrix}_{N_g \times 1}.$$

The unknown channel vector $\boldsymbol{g}_1$ represents multipath propagation and other distortions.

III. Background

Here, the linear detection of DS-CDMA systems, the MOE detector, and the IQRD-RLS algorithm are briefly outlined.

A. Linear Detection

The linear detector output is a linear combination of the received chip sampled signals. Thus,

$$\boldsymbol{y}(n) = \boldsymbol{f}^H(n)\boldsymbol{x}(n). \tag{7}$$

The output of the detector is $\boldsymbol{y}(n)$ and $\boldsymbol{f}^H(n)$ is a $N_f \times 1$ vector consisting of the weights. In BPSK, the bit decision is made according to

$$\hat{\boldsymbol{s}}_1(n) = \operatorname{sgn}\left(\operatorname{Re}\left\{\boldsymbol{y}_1(n)\right\}\right). \tag{8}$$

The detector output energy is given by

$$E\left\{\left|\boldsymbol{y}(n)\right|^2\right\} = E\left\{\left|\boldsymbol{f}^H\boldsymbol{x}(n)\right|^2\right\} = \boldsymbol{f}^H\boldsymbol{R}_{xx}\boldsymbol{f} \tag{9}$$

where $\boldsymbol{R}_{xx}(n) = E\{\boldsymbol{x}(n)\boldsymbol{x}^H(n)\}$ is the data covariance matrix.

B. MOE Detector

The MOE linear detector can be obtained by minimizing the output energy of the receiver subject to a certain number of constraints to avoid the cancellation of the interested user signal scattered in different multipaths during the minimization of the detector output energy. Therefore, the constrained optimization approach constructively ensemble the multipath components instead of suppressing them. We can generally impose a set of linear constraints of the form $\boldsymbol{C}_1^H\boldsymbol{f} = \boldsymbol{g}$, where $\boldsymbol{g}$ is a $N_g \times 1$ general parameter vector to be determined. Thus, the optimal MOE detector can be obtained by solving the following constrained minimization problem [3]–[9]:

$$\min_{\boldsymbol{f}} \boldsymbol{f}^H\boldsymbol{R}_{xx}\boldsymbol{f} \text{ subject to } \boldsymbol{C}_1^H\boldsymbol{f} = \boldsymbol{g}. \tag{10}$$

The solution to the constrained optimization problem (10) is then of the form

$$\boldsymbol{f} = \boldsymbol{R}_{xx}^{-1}\boldsymbol{C}_1\left(\boldsymbol{C}_1^H\boldsymbol{R}_{xx}^{-1}\boldsymbol{C}_1\right)^{-1}\boldsymbol{g}. \tag{11}$$

The optimal constrained vector $\boldsymbol{g}_{\text{opt}}$ can be obtained by comparing (11) with the nonblind MMSE detector (i.e., $\boldsymbol{f} = \boldsymbol{R}_{xx}^{-1}\boldsymbol{C}_1\boldsymbol{g}_1$) [5]. Therefore, the optimum choice for $\boldsymbol{g}$ is $\boldsymbol{C}_1^H\boldsymbol{R}_{xx}^{-1}\boldsymbol{C}_1\boldsymbol{g}_1$, which requires knowledge of the channel parameters $\boldsymbol{g}_1$ which may not be available in a blind detection. Alternatively, we can optimize $\boldsymbol{g}$ by maximizing the power of the MOE receiver after the interfering users have been discarded by substituting (11) into (10), which yields [3]

$$\max_{\|\boldsymbol{g}\|=1} \boldsymbol{f}^H\boldsymbol{R}_{xx}\boldsymbol{f} = \max_{\|\boldsymbol{g}\|=1} \boldsymbol{g}^H\left(\boldsymbol{C}_1^H\boldsymbol{R}_{xx}^{-1}\boldsymbol{C}_1\right)^{-1}\boldsymbol{g}. \tag{12}$$

Therefore, the optimal max/min constrained vector $\boldsymbol{g}_{\max/\min}$ is the eigenvector of $(\boldsymbol{C}_1^H\boldsymbol{R}_{xx}^{-1}\boldsymbol{C}_1)^{-1}$ corresponding to the maximum eigenvalue. This approach has a significant improvement in handling the multipath at high SNR [3].

C. IQRD-RLS Algorithm

The IQRD-RLS algorithm is exploited to update the inverse *Cholesky* factor $\boldsymbol{R}^{-H}(n)$ of the covariance matrix of the received vector $\boldsymbol{x}(n)$. Let us start by the QR decomposition of $\boldsymbol{R}_{xx}$, which is given by

$$\boldsymbol{R}_{xx} = \boldsymbol{R}^H(n)\boldsymbol{R}(n). \tag{13}$$

A rotation matrix $\boldsymbol{P}(n)$ can be found to update the inverse *Cholesky* factor according to the following equations (see [10] and [11] for more details on the IQRD-RLS algorithm):

$$\begin{bmatrix} \boldsymbol{R}^{-H}(n) \\ \boldsymbol{j}^H(n) \end{bmatrix} = \boldsymbol{P}(n)\begin{bmatrix} \frac{\boldsymbol{R}^{-H}(n-1)}{\sqrt{\lambda}} \\ \boldsymbol{0}_{N_f}^T \end{bmatrix} \tag{14}$$

where $\boldsymbol{j}(n) = \boldsymbol{R}^{-H}(n-1)\boldsymbol{a}(n)/\sqrt{\lambda}b(n)$ and λ is a scalar forgetting factor.

It can be shown that $\boldsymbol{P}(n)$ is an $(N_f+1)\times(N_f+1)$ orthogonal matrix (i.e., $\boldsymbol{P}(n)\boldsymbol{P}^H(n) = I_{N_f+1}$) which successively annihilates the elements of an $N_f \times 1$ intermediate vector $\boldsymbol{a}(n) = \boldsymbol{R}^{-H}(n-1)\boldsymbol{x}(n)\sqrt{\lambda}$ from the top by rotating them into a related Kalman gain value $b(n)$ using a sequence of *Givens rotation*, i.e.,

$$\boldsymbol{P}(n)\begin{bmatrix} \boldsymbol{a}(n) \\ 1 \end{bmatrix} = \begin{bmatrix} \boldsymbol{0}_{N_f} \\ b(n) \end{bmatrix}. \tag{15}$$

The Kalman gain can be calculated by scaling the vector $\boldsymbol{j}(n)$ by $b(n)$, where the vector $\boldsymbol{j}(n)$ and $b(n)$ are computed using the Givens rotations, when $\boldsymbol{R}^{-H}(n)$ is updated from $\boldsymbol{R}^{-H}(n-1)$ [11]. The derivation of the IQRD algorithm is comprehensively provided in [10] and [11], and it will be further clarified during systolic implementation in Section VI. It has been shown in [24] that the recursive update of the triangular matrix (i.e., Kalman gain estimate) of the IQRD-RLS algorithm requires $O(N_f)$ operations.

Givens rotation is the most commonly used method in performing QRD and IQRD updating. The generic formula for these rotations requires explicit square-root (sqrt) computations which constitute a computational bottleneck and are quite undesirable from the practical VLSI circuit design point of view [25]. More specifically, in VLSI circuit design, sqrt operation is expensive, because it takes up a large area or is slow. Therefore, avoiding or minimize sqrt operations is preferred. Thus, much effort has been spent on minimizing or even eliminating the sqrt operation from the Givens rotations method. A unified systematic approach for the sqrt-free Givens rotations is provided in [25] and references therein.

IV. Optimal MOE-IQRD Receiver With Max/Min Approach

We start from the optimal equation of the weight vector (11) and, using (13), the optimal MOE detector is then given by

$$\boldsymbol{f}(n) = \left[\boldsymbol{R}^H(n)\boldsymbol{R}(n)\right]^{-1}\boldsymbol{C}_1\left\{\boldsymbol{C}_1^H\left[\boldsymbol{R}^H(n)\boldsymbol{R}(n)\right]^{-1}\boldsymbol{C}_1\right\}^{-1}\boldsymbol{g}. \tag{16}$$

We define two new matrices as follows. $\boldsymbol{\Delta}(n) = [\boldsymbol{R}^H(n)\boldsymbol{R}(n)]^{-1}\boldsymbol{C}_1$ is a $N_f \times N_g$ matrix, and $\boldsymbol{\Pi}(n) = \boldsymbol{C}_1^H\boldsymbol{\Delta}(n)$ is a $N_g \times N_g$ matrix, and, in turn, the optimal weight vector can be expressed as

$$\boldsymbol{f}(n) = \boldsymbol{\Delta}(n)\boldsymbol{\Pi}^{-1}(n)\boldsymbol{g}. \tag{17}$$

The algorithm is developed by deriving a recursive update equation for $\boldsymbol{\Delta}(n)$ and $\boldsymbol{\Pi}^{-1}(n)$ and, consequently, the optimal weight vector $\boldsymbol{f}(n)$ can be updated recursively.

Using the update of the inverse *Cholesky factor* in (14) and multiplying each side with its Hermitian transpose, an update equation for the data covariance matrix is obtained as

$$\boldsymbol{R}^{-1}(n)\boldsymbol{R}^{-H}(n) = \frac{\boldsymbol{R}^{-1}(n-1)\boldsymbol{R}^{-H}(n-1)}{\lambda} - \boldsymbol{j}(n)\boldsymbol{j}^{H}(n). \tag{18}$$

Postmultiplying (18) by $\boldsymbol{C}_1$, a recursive formula for $\boldsymbol{\Delta}(n)$ matrix is obtained as follows:

$$\boldsymbol{\Delta}(n) = \lambda^{-1}\boldsymbol{\Delta}(n-1) - \boldsymbol{j}(n)\boldsymbol{\pi}^{H}(n) \tag{19}$$

where

$$\boldsymbol{\pi}(n) = \boldsymbol{C}_1^{H}\boldsymbol{j}(n). \tag{20}$$

Premultiplying (19) by $\boldsymbol{C}_1^{H}$, a recursive formula for the matrix $\boldsymbol{\Pi}(n)$ is obtained as follows:

$$\boldsymbol{\Pi}(n) = \lambda^{-1}\boldsymbol{\Pi}(n-1) - \boldsymbol{\pi}(n)\boldsymbol{\pi}^{H}(n). \tag{21}$$

By applying the matrix inversion lemma [26] to (21), we get

$$\boldsymbol{\Pi}^{-1}(n) = \lambda\boldsymbol{\Pi}^{-1}(n-1) + \frac{\lambda^2\boldsymbol{\Pi}^{-1}(n-1)\boldsymbol{\pi}(n)\boldsymbol{\pi}^{H}(n)\boldsymbol{\Pi}^{-1}(n-1)}{1-\lambda\boldsymbol{\pi}^{H}(n)\boldsymbol{\Pi}^{-1}(n-1)\boldsymbol{\pi}(n)}. \tag{22}$$

Therefore, the recursive formulas for both $\boldsymbol{\Delta}(n)$ and $\boldsymbol{\Pi}^{-1}(n)$ matrices have been derived. A recursive formula for the optimal adaptive detector $\boldsymbol{f}(n)$ in (17) can be obtained by substituting (19) and (22) into (17). A direct-form MOE detector with fixed constraints (i.e., without max/min approach) can be obtained by setting $\boldsymbol{g} = \boldsymbol{1}_{N_g}$ (i.e., equal gain combining for multipath channel components). Equations (17), (19), and (22) form the basis for this detector.

Consider now the MOE in (16) with the max/min approach addressed in Section III-B, the optimized constrained vector $\boldsymbol{g}(n)$ can be derived analogs to (12) as follows

$$\max_{\|\boldsymbol{g}\|=1} \boldsymbol{f}_{\max/\min}^{H}\bar{\boldsymbol{R}}^{H}(n)\bar{\boldsymbol{R}}(n)\boldsymbol{f}_{\max/\min}. \tag{23}$$

Substituting (17) into (23), it can be shown that the optimal solution (i.e., $\boldsymbol{g}_{\max/\min}$) is $\boldsymbol{v}_1$, and the principal eigenvector corresponding to the maximum eigenvalue of the matrix $\boldsymbol{\Pi}^{-1}(n)$ or the minor eigenvector $\boldsymbol{\gamma}_1$ corresponding to the minimum eigenvalue of matrix $\boldsymbol{\Pi}(n)$, and then the corresponding optimal max/min weight vectors can be, respectively, expressed in the following forms:

$$\boldsymbol{f}_{\max/\min} = \beta_1\boldsymbol{\Delta}(n)\boldsymbol{v}_1 \tag{24}$$

$$\boldsymbol{f}_{\max/\min} = \frac{1}{\alpha_1}\boldsymbol{\Delta}(n)\boldsymbol{\gamma}_1 \tag{25}$$

where β_1 and α_1 are the maximum and the minimum eigenvalues of $\boldsymbol{\Pi}^{-1}(n)$ and $\boldsymbol{\Pi}(n)$, respectively. It is noteworthy to highlight that the multiplication of the receiver coefficients vector by any positive constant does not affect the bit-error-rate (BER) probability of the detector output. Therefore, the two constants β_1 and α_1 are immaterial constants.

A recursive formula for updating matrix $\boldsymbol{\Delta}(n)$ is derived in (19). Therefore, a complete IQRD-RLS recursive implementation of the max/min optimal weight vector using the IQRD method can be obtained by recursively updating the principle eigenvector of $\boldsymbol{\Pi}^{-1}(n)$ or the minor eigenvector of $\boldsymbol{\Pi}(n)$ using an IQRD-RLS-based subspace tracking algorithm.

In order to pursue the principal component of the target matrix $\boldsymbol{\Pi}^{-1}(n)$ using subspace tracking algorithms as in [27] and [28], it should be formulated in the weighted sample average format, i.e.,

$$\boldsymbol{\Pi}^{-1}(n) = \sum_{i=1}^{n}\lambda^{n-i}\boldsymbol{d}(i)\boldsymbol{d}^{H}(i) \tag{26}$$

where λ is the usual forgetting factor with $0 \ll \lambda \leq 1$ and $\boldsymbol{d}(i)$ is a sequence of $N_g \times 1$ unknown vectors to be determined. Alternatively, it can be updated using the following well-known recursive formula:

$$\boldsymbol{\Pi}^{-1}(n) = \lambda\boldsymbol{\Pi}^{-1}(n-1) + \boldsymbol{d}(n)\boldsymbol{d}^{H}(n). \tag{27}$$

By comparing (22) with (27), the unknown vector $\boldsymbol{d}(n)$ can be obtained as follows:

$$\boldsymbol{d}(n) = \frac{\lambda\boldsymbol{\Pi}^{-1}(n-1)\boldsymbol{\pi}(n)}{\sqrt{1-\lambda\boldsymbol{\pi}^{H}(n)\boldsymbol{\Pi}^{-1}(n-1)\boldsymbol{\pi}(n)}}. \tag{28}$$

An orthogonal subspace tracking algorithm can be employed to track the Principle Component (PC) $\boldsymbol{v}_1$ of $\boldsymbol{\Pi}^{-1}(n)$ and hence the optimal max/min weight vector can be estimated using (24). For example, the orthogonal version of the projection approximation subspace tracking (OPASTd) or the normalized orthogonal OJA (NOOJA), addressed respectively in [27] and [28], can be used for tracking the principal component (PC). The orthogonal versions are preferred to ensure the normalization of the estimated principal component (i.e., $\boldsymbol{v}_1^{H}\boldsymbol{v}_1 = 1$) during recursive implementation of the subspace tracking algorithm. Specifically, the orthogonal subspace tracking algorithms guarantee the orthogonality of the weight matrix, which consists of the principal subspace and thus guarantees the normalization of each eigenvector inside the principal subspace.

Tracking the minor component (MC) requires a lower computational complexity than tracking the PC, where the matrix $\boldsymbol{\Pi}(n)$ is used instead of its inverse. However, due to the instability in tracking the MC, an alternative approach is adopted for tracking the MC of the matrix $\boldsymbol{\Pi}(n)$ (see [16] and [17]). The new approach depends on the matrix itself rather than its update form. We start by forming the following real-valued Lagrangian function [29]

$$\boldsymbol{\Psi}_n(\boldsymbol{g},\zeta) = \boldsymbol{g}^{H}(n-1)\boldsymbol{\Pi}(n)\boldsymbol{g}(n-1) + \frac{1}{2}\zeta(n)\left(1-\boldsymbol{g}^{H}(n-1)\boldsymbol{g}(n-1)\right). \tag{29}$$

The optimal channel vector $\boldsymbol{g}$ (i.e., an estimation of the minor eigenvector $\boldsymbol{v}_1$) can be obtained by minimizing (29), and hence the channel vector can be updated as follows:

$$\boldsymbol{g}(n) = \boldsymbol{g}(n-1) - \mu\nabla_{\boldsymbol{g}}\boldsymbol{\Psi}_n(\boldsymbol{g},\zeta). \tag{30}$$

From (29), the gradient vector $\boldsymbol{z}(n) = \nabla_{\boldsymbol{g}} \boldsymbol{\Psi}_n(\boldsymbol{g}, \zeta)$ can be computed as follows:

$$\boldsymbol{z}(n) = \boldsymbol{\Pi}(n)\boldsymbol{g}(n-1) - \zeta(n)\boldsymbol{g}(n-1). \tag{31}$$

The step-size should be set to a suitable value that guarantees faster convergence. Further improvement to this method can be achieved by updating the step-size on the basis of optimal estimation in terms of convergence speed. The optimal step-size can be calculated using an approach similar to the one introduced in [6] and [27]. Substituting (30) into (29) and incorporating a variable step-size $\mu(n)$ into (30) instead of the fixed step-size and omitting the second term for a moment, the cost function determined at $n+1$ snapshot is obtained as follows:

$$\begin{aligned}\boldsymbol{\Psi}_{n+1}(\boldsymbol{g}, \zeta) = \boldsymbol{\Psi}_n(\boldsymbol{g}, \zeta) &- 2\mu(n)\boldsymbol{g}^H(n-1)\boldsymbol{\Pi}(n)\boldsymbol{z}(n) \\ &+ \mu^2(n)\boldsymbol{z}^H(n)\boldsymbol{\Pi}(n)\boldsymbol{z}(n).\end{aligned} \tag{32}$$

Therefore, the optimal step size that guarantees faster convergence speed can be obtained by differentiating (32) with respect to the adaptive step-size $\mu(n)$ and setting the result to zero. Assuming that $\boldsymbol{\Psi}_n(\boldsymbol{g}, \zeta)$ is independent of $\mu(n)$, then the optimal step-size can be derived as follows:

$$\mu_{opt}(n) = \frac{\chi \boldsymbol{g}^H(n-1)\boldsymbol{\Pi}(n)\boldsymbol{z}(n)}{\boldsymbol{z}^H(n)\boldsymbol{\Pi}(n)\boldsymbol{z}(n) + \eta}. \tag{33}$$

The two positive constants χ and η are added to control the numerical stability of the algorithm [28]. The second term in (29) cannot affect (33), as it is equal to zero if the normalization of the channel vector during the update process is guaranteed.

Assume that the previous estimated channel vector $\boldsymbol{g}(n-1)$ satisfies the normalization constraint, and then its update $\boldsymbol{g}(n)$ should also satisfy the normalization constraint in (29). A closed-form expression for the Lagrange multiplier $\zeta(n)$ can be obtained by plugging (31) into (30) and then substituting (30) into the normalization constraint, i.e.,

$$\boldsymbol{g}^H(n)\boldsymbol{g}(n) = 1. \tag{34}$$

Consequently, and after some manipulations, we have

$$a\zeta^2(n) - 2b\zeta(n) + c \tag{35}$$

where

$$\begin{aligned} a &= \mu_{opt}(n-1) \\ b &= 1 + \mu_{opt}(n-1)\boldsymbol{g}^H(n-1)\boldsymbol{\Pi}(n)\boldsymbol{g}(n-1) \\ c &= \mu_{opt}(n-1)\boldsymbol{g}^H(n-1)\boldsymbol{\Pi}^2(n)\boldsymbol{g}(n-1) \\ &\quad + 2\boldsymbol{g}^H(n-1)\boldsymbol{\Pi}(n)\boldsymbol{g}(n-1). \end{aligned} \tag{36}$$

Therefore, the Lagrange multiplier $\zeta(n)$ can be expressed as:

$$\zeta(n) = \frac{-b \pm \sqrt{b^2 - ac}}{a}. \tag{37}$$

It is easily verified that $b^2 > ac$. As a result, the roots of the quadratic equation (35) are two real roots. The smaller root is selected to ensure algorithm stability. Finally, a recursive implementation of (25) can be found by substituting (19) and (30) into (25). The channel vector in (30) is considered as an optimal estimation of the minor eigenvector $\boldsymbol{v}_1$.

TABLE I
SUMMARY OF OPTIMAL ROBUST MOE RECEIVER WITH MAX/MIN APPROACH AND QIC

- Initialization:
  - $\boldsymbol{R}^{-H}(0) = \boldsymbol{I}_{N_f}$, $\boldsymbol{\Lambda}(0) = \boldsymbol{R}^{-1}(0)\boldsymbol{R}^{-H}(0)\boldsymbol{C}_1$, $\boldsymbol{\Pi}^{-1}(0) = \left[\boldsymbol{C}_1^H \boldsymbol{\Lambda}(0)\right]^{-1}$
  - select $\boldsymbol{g}(0)$ to be any normalized vector
  - $\boldsymbol{f}_{\max/\min}(0) = \hat{\boldsymbol{f}}_{\max/\min}(0) = \boldsymbol{\Lambda}(0)\boldsymbol{g}(0)$, $\mu_{opt}(0) = 0.001$
- For $n = 1, 2, \mathrm{L}$, do:
  - Update $\boldsymbol{R}^{-H}(n)$ using $\begin{bmatrix} \boldsymbol{R}^{-H}(n) \\ \boldsymbol{j}^H(n) \end{bmatrix} = \boldsymbol{P}(n) \begin{bmatrix} \frac{\boldsymbol{R}^{-H}(n-1)}{\sqrt{\lambda}} \\ 0^T \end{bmatrix}$; $6N_f$
  - where $\boldsymbol{P}(n) \begin{bmatrix} \boldsymbol{a}(n) \\ 1 \end{bmatrix} = \begin{bmatrix} 0 \\ b(n) \end{bmatrix}$ and $\boldsymbol{a}(n) = \frac{\boldsymbol{R}^{-H}(n-1)x(n)}{\sqrt{\lambda}}$.
  - Update the covariance matrix ➔ $\boldsymbol{R}_{xx}^{-1}(n) = \frac{\boldsymbol{R}_{xx}^{-1}(n-1)}{\lambda} - \boldsymbol{j}(n)\boldsymbol{j}^H(n)$; N_f^2
  - Update the $\boldsymbol{\Lambda}(n)$ matrix ➔ $\boldsymbol{\Lambda}(n) = \lambda^{-1}\boldsymbol{\Lambda}(n-1) - \boldsymbol{j}(n)\boldsymbol{\pi}^H(n)$; $2N_f N_g$
  - Update the $\boldsymbol{\Pi}(n)$ matrix ➔ $\boldsymbol{\Pi}(n) = \frac{1}{\lambda}\boldsymbol{\Pi}(n-1) - \boldsymbol{\pi}^H(n)\boldsymbol{\pi}(n)$; N_g^2
  - *Channel vector tracking:*
    - $a = \mu_{opt}(n-1)$
    - $b = 1 + \mu_{opt}(n-1)\boldsymbol{g}^H(n-1)\boldsymbol{\Pi}(n)\boldsymbol{g}(n-1)$; $N_g^2 + N_g$
    - $c = \mu_{opt}(n-1)\boldsymbol{g}^H(n-1)\boldsymbol{\Pi}^2(n)\boldsymbol{g}(n-1) + 2\boldsymbol{g}^H(n-1)\boldsymbol{\Pi}(n)\boldsymbol{g}(n-1)$; N_g
    - $\zeta(n) = \frac{-b - \sqrt{b^2 - \mu_{opt}(n-1)c}}{\mu_{opt}(n-1)}$; *Lagrange multiplier*
    - $\boldsymbol{z}(n) = \boldsymbol{\Pi}(n)\boldsymbol{g}(n-1) - \zeta(n)\boldsymbol{g}(n-1)$; *gradient vector estimation*
    - $\mu_{opt}(n) = \frac{\sigma \boldsymbol{g}^H(n-1)\boldsymbol{\Pi}(n)\boldsymbol{z}(n)}{\boldsymbol{z}^H(n)\boldsymbol{\Pi}(n)\boldsymbol{z}(n) + \eta}$; $N_g^2 + 2N_g$ *optimum step-size*
    - $\boldsymbol{g}(n) = \boldsymbol{g}(n-1) - \mu_{opt}(n)\boldsymbol{z}(n)$; *estimated channel vector*
  - $\boldsymbol{f}_{\max/\min}(n) = \boldsymbol{\Lambda}(n)\boldsymbol{g}(n)$; $N_f N_g$; *optimal MOE detector with max/min approach*
  - *Robust Detector with QIC (VL Technique)*
  - if $\left\|\boldsymbol{f}_{\max/\min}(n)\right\|^2 > \rho$ (QIC)
    - $\tilde{\boldsymbol{f}}_{\max/\min}(n) = \boldsymbol{R}_{xx}^{-1}(n)\boldsymbol{f}_{\max/\min}(n)$; N_f^2
    - $a_1 = \boldsymbol{f}_{\max/\min}{}^H(n)\boldsymbol{f}_{\max/\min}(n)$; N_f
    - $b_1 = -2\,\mathrm{Re}\left\{\boldsymbol{f}_{\max/\min}{}^H(n)\tilde{\boldsymbol{f}}_{\max/\min}(n)\right\}$; N_f
    - $c_1 = \tilde{\boldsymbol{f}}_{\max/\min}{}^H(n)\tilde{\boldsymbol{f}}_{\max/\min}(n) - \rho$; N_f
    - $\varepsilon = \frac{-b_1 \pm \mathrm{Re}\left\{\sqrt{b_1^2 - 4a_1c_1}\right\}}{2a_1}$
    - $\hat{\boldsymbol{f}}_{\max/\min} \approx \boldsymbol{f}_{\max/\min} - \varepsilon\tilde{\boldsymbol{f}}_{\max/\min}$; *robust MOE detector with QIC*
  - else
    - $\hat{\boldsymbol{f}}_{\max/\min} = \boldsymbol{f}_{\max/\min}$, $\varepsilon = 0$
  - end if
- End for

The Lagrange method addressed in this section can be used for tracking the principal component of the matrix $\boldsymbol{\Pi}^{-1}(n)$ by replacing the matrix $\boldsymbol{\Pi}(n)$ in (29) with $\boldsymbol{\Pi}^{-1}(n)$ and maximizing the ensuing cost function instead of minimizing it. Therefore, a recursive update formula for (24) can be obtained as well. The final optimal MOE detector with minor subspace tracking is summarized in Table I. As shown in Table I, the total multiplications complexity of the proposed optimal MOE algorithm is $O(3N_g^2 + 2N_fN_g + 4N_g + 6N_f)$.

V. Adaptive Implementation of Robust MOE Receivers at Low SNR Using the IQRD-RLS Algorithm

In order to analyze the performance of the recently emerged robust MOE detectors at low SNR, we have to scrutinize their output SINR. For any linear MUD receiver, the output SINR can be expressed in the following form (see [3], [5], and [23]):

$$\mathrm{SINR} = \frac{\boldsymbol{f}^H \boldsymbol{h}_1 \boldsymbol{h}_1^H \boldsymbol{f}}{\boldsymbol{f}^H \boldsymbol{R}_{\boldsymbol{xx}} \boldsymbol{f} - \boldsymbol{f}^H \boldsymbol{h}_1 \boldsymbol{h}_1^H \boldsymbol{f}} \tag{38}$$

where the data covariance matrix $\boldsymbol{R}_{\boldsymbol{xx}}$ can be expressed as $\boldsymbol{R}_{xx} = (\boldsymbol{h}_1\ \boldsymbol{H}_i)(\boldsymbol{h}_1\ \boldsymbol{H}_i)^H + \sigma_w^2 \boldsymbol{I}_{N_f}$.

The optimal max/min MOE detector incorporates two optimization processes. Initially, the output power of the receiver is minimized under code-constraining to suppress interfering users and preclude the interested user from cancellation. Second, the power of the receiver is maximized after interference has been cancelled. Pragmatically, the two processes are concurrently conducted during adaptive implementation. However, and without loss of generality, the two processes are proposed to be successively implemented. As a consequence, after the minimization process, the output SINR can be expressed as

$$\mathrm{SINR} = \frac{\boldsymbol{f}_{\min}^H \boldsymbol{h}_1 \boldsymbol{h}_1^H \boldsymbol{f}_{\min}}{\sigma_w^2 \boldsymbol{f}_{\min}^H \boldsymbol{f}_{\min} + \omega} \tag{39}$$

where ω represents the residual interference component and $\boldsymbol{f}_{\min}$ stands for the detector parameters after the minimization process (i.e., interference cancellation).

The max/min channel estimation that is procured by maximization of the receiver output power after the interference has been rejected can be expressed as the following optimization problem:

$$\max_{\boldsymbol{f}_{\max/\min}} \Big(\boldsymbol{f}_{\max/\min}^H \boldsymbol{h}_1 \boldsymbol{h}_1^H \boldsymbol{f}_{\max/\min} + \sigma_w^2 \boldsymbol{f}_{\max/\min}^H \boldsymbol{f}_{\max/\min} + \omega \Big). \tag{40}$$

Therefore, a performance degradation in the output SINR arises due to the maximization in (40) does not oversee the noise term $\sigma_w^2 \boldsymbol{f}_{\max/\min}^H \boldsymbol{f}_{\max/\min}$. More preciously, the optimal constrained MOE detector with the max/min approach experiences some performance degradation because the optimal constraint vector $\boldsymbol{g}_{\max/\min}$ is a perturbed channel vector [3]. The perturbation depends on the background noise; it cannot be neglected especially at low SNR. Several approaches have been developed to overcome noise enhancement at low SNR during max/min optimization. In the subsequent sections, these approaches are summarized and implemented using the IQRD-RLS algorithm.

A. Noise Cancellation Schemes

In these techniques, the contribution of the noise is partially subtracted from the cost function [7] or completely eradicated if the noise power can be precisely estimated [8]. In the following two sections, the preceding two techniques are presented respectively.

1) Improved Cost Function: An improved cost function is developed in [7] based on the relation between the constrained optimization approach and the subspace approach. The new cost function along with its IQRD implementation can be expressed as follows:

$$\begin{aligned} \tilde{\boldsymbol{g}} &= \arg\min_{\|\tilde{\boldsymbol{g}}\|=1} \tilde{\boldsymbol{g}}^H \left(\boldsymbol{C}_1^H \boldsymbol{R}_{xx}^{-1} \boldsymbol{C}_1 - \lambda_{\min} \boldsymbol{C}_1^H \boldsymbol{C}_1 \right) \tilde{\boldsymbol{g}} \\ &= \arg\min_{\|\tilde{\boldsymbol{g}}\|=1} \tilde{\boldsymbol{g}}^H \left(\boldsymbol{\Pi}(n) - \lambda_{\min} \boldsymbol{C}_1^H \boldsymbol{C}_1 \right) \tilde{\boldsymbol{g}} \end{aligned} \tag{41}$$

where $\lambda_{\min}$ is the reciprocal of the largest eigenvalue of $\boldsymbol{R}_{xx}$.

Therefore, the improved channel vector $\tilde{\boldsymbol{g}}$ can be estimated using the IQRD-RLS method as the eigenvector corresponding to the smallest eigenvalue of the second cost function in (41). The Lagrange method proposed in Section IV can be employed to track the improved channel vector.

2) Modified Cost Function: In order to completely mitigate the noise effect and obtain an unbiased estimation of the channel vector, a new cost function is formed in [8] by removing the noise contribution from the data covariance matrix as follows:

$$\overline{\boldsymbol{R}}_{xx} = \boldsymbol{R}_{xx} - \tau \sigma_w^2 \boldsymbol{I}_{N_f} \tag{42}$$

where τ quantifies the extent of the noise mitigation and should satisfy $0 \le \tau < 1$ to ensure that the modified covariance matrix $\overline{\boldsymbol{R}}_{xx}$ is positive definite.

Following the max/min approach described before, the modified channel vector $\overline{\boldsymbol{g}}$ can be obtained as

$$\begin{aligned} \overline{\boldsymbol{g}} &= \arg\min_{\|\overline{\boldsymbol{g}}\|=1} \overline{\boldsymbol{g}}^H \left(\boldsymbol{C}_1^H \overline{\boldsymbol{R}}_{xx}^{-1} \boldsymbol{C}_1 \right) \overline{\boldsymbol{g}} \\ &\triangleq \arg\min_{\|\overline{\boldsymbol{g}}\|=1} \overline{\boldsymbol{g}}^H \left(\left[\boldsymbol{C}_1^H + \tau \sigma_w^2 \boldsymbol{\Delta}^H(n) \right] \boldsymbol{\Delta}(n) \right) \overline{\boldsymbol{g}}. \end{aligned} \tag{43}$$

The noise power σ_w^2 can be estimated from the smallest eigenvalue of the data covariance matrix. The second optimization in (43) can be verified using a Taylor series approximation of $[\boldsymbol{I}_{N_f} - \tau \sigma_w^2 \overline{\boldsymbol{R}}_{xx}^{-1}(n)]^{-1}$. Similarly, the proposed Lagrange method in Section IV can be used to track the modified channel vector $\overline{\boldsymbol{g}}$. It is noteworthy that this method assumes perfect covariance matrix estimation. More specifically, if the actual covariance matrix is used, this method performs similarly to the nonblind MMSE detector. Otherwise, imperfect covariance matrix estimation dramatically degrades the performance of this method.

B. Capon Method

The Capon method is based on the estimation of the channel vector using a generalized eigenvalue decomposition problem. In [2], a procedure evocative to the Capon estimation method is proposed for optimizing the MOE power as a function of the effective signature waveform subject to effective signature waveform normalization constraint (i.e., $\|\boldsymbol{h}_1\| = 1$, that is,

$$\begin{aligned} \hat{\boldsymbol{g}} &= \arg\max_{\substack{\boldsymbol{h}_1 = \boldsymbol{C}_1 \hat{\boldsymbol{g}} \\ \|\boldsymbol{h}_1\|=1}} \frac{\boldsymbol{h}_1^H \boldsymbol{h}_1}{\boldsymbol{h}_1^H \boldsymbol{R}_{xx}^{-1} \boldsymbol{h} 1} \\ &= \arg\min_{\hat{\boldsymbol{g}}} \frac{\hat{\boldsymbol{g}}^H \boldsymbol{C}_1^H \boldsymbol{R}_{xx}^{-1} \boldsymbol{C}_1 \hat{\boldsymbol{g}}}{\hat{\boldsymbol{g}}^H \boldsymbol{C}_1^H \boldsymbol{C}_1 \hat{\boldsymbol{g}}} = \arg\min_{\hat{\boldsymbol{g}}} \frac{\hat{\boldsymbol{g}}^H \boldsymbol{\Pi}(n)_1 \hat{\boldsymbol{g}}}{\hat{\boldsymbol{g}}^H \mathbb{C} \hat{\boldsymbol{g}}} \end{aligned} \tag{44}$$

where $\boldsymbol{h}_1 = \boldsymbol{C}_1\hat{\boldsymbol{g}}$ and $\mathbb{C} = \boldsymbol{C}_1^H\boldsymbol{C}_1$. Therefore, the third optimization problem in (44) is equivalent to a generalized eigenvalue problem involving the pensile of $(\boldsymbol{\Pi}(n), \mathbb{C})$. A recursive formula for the Capon channel vector can be obtained as follows [32]:

$$\hat{\boldsymbol{g}}(n) = \kappa\boldsymbol{\Pi}^{-1}(n)\mathbb{C}\hat{\boldsymbol{g}}(n-1) \tag{45}$$

where $\kappa = \hat{\boldsymbol{g}}^H(n-1)\boldsymbol{\Pi}(n)\hat{\boldsymbol{g}}(n-1)/\hat{\boldsymbol{g}}^H(n-1)\mathbb{C}\hat{\boldsymbol{g}}(n-1)$ is an immaterial constant.

C. Power of $\boldsymbol{R}$ Receiver (POR)

It is verified in [3] that the channel estimation error $\boldsymbol{g}_{\max/\min} - \boldsymbol{g}_1/\|\boldsymbol{g}_1\|$ is proportional to the noise power σ_w^2 which is the smallest eigenvalue of $\boldsymbol{R}_{xx}$. Therefore, boosting the power of $\boldsymbol{R}_{xx}$ (POR) in the MOE cost function makes the minimum eigenvalue of the ensuing matrix (i.e., $\boldsymbol{R}_{xx}^{-m}$) decrease exponentially. Consequently, the channel estimation error is expected to decrease as well [9]. Following this direction, the POR channel estimation method can be formulated as follows:

$$\begin{aligned}\breve{\boldsymbol{g}} &= \arg\min_{\substack{\|\boldsymbol{g}\|=1\\ m\geq 2}} \breve{\boldsymbol{g}}^H\left(\boldsymbol{C}_1^H\boldsymbol{R}_{xx}^{-m}\boldsymbol{C}_1\right)\breve{\boldsymbol{g}}\\ &\underset{m=2}{\Rightarrow} \arg\min_{\|\boldsymbol{g}\|=1} \breve{\boldsymbol{g}}^H\left(\boldsymbol{C}_1^H\boldsymbol{R}_{xx}^{-H}\boldsymbol{R}_{xx}^{-1}\boldsymbol{C}_1\right)\breve{\boldsymbol{g}}\\ &= \arg\min_{\|\boldsymbol{g}\|=1} \breve{\boldsymbol{g}}^H\left(\boldsymbol{\Delta}^H(n)\boldsymbol{\Delta}(n)\right)\breve{\boldsymbol{g}}\end{aligned} \tag{46}$$

Further discussion on this method and its adaptive implementation using the RLS algorithm is provided in [9]. In this paper, the POR receiver is implemented using the third optimization problem in (46) using the IQRD-RLS algorithm with the proposed Lagrange method.

D. Max/Min With QIC Approach

In order to mitigate the effect of noise enhancement at low SNR, we can impose a QIC on the weight vector norm during the maximization process [5], [6]. To start the formulation of this detector, we directly impose the QIC on the maximization portion of the max/min optimization process, i.e.,

$$\begin{aligned}\max_{\|\boldsymbol{g}\|=1}\Bigg\{&\min_{\boldsymbol{f}_{\max/\min}}\left\{\boldsymbol{f}_{\max/\min}^H\boldsymbol{R}_{xx}\boldsymbol{f}_{\max/\min}\right\}\\ &\text{subject to } \boldsymbol{C}_1^H\boldsymbol{f}_{\max/\min} = \boldsymbol{g}\Bigg\}\\ \text{subject to}\quad &\boldsymbol{f}_{\max/\min}^H\boldsymbol{f}_{\max/\min} \leq \rho\end{aligned} \tag{47}$$

where ρ is the constrained value and should be precisely set to an appropriate value. A similar approach was proposed in [30] and [31] with a beamforming application using single constraint optimization rather than multiple constraints. The solution of this optimization problem can be acquired by solving the inner optimization problem as in (10) and then solving the outer optimization problem using the Lagrange method. As a result, the max/min optimal detector with strength against noise enhancement at low SNR can be expressed as

$$\hat{\boldsymbol{f}}_{\max/\min} = (\boldsymbol{R}_{xx} + \varepsilon I)^{-1}\boldsymbol{C}_1\boldsymbol{g}_{\max/\min}. \tag{48}$$

The normalized channel vector $\boldsymbol{g}_{\max/\min}$ can be obtained using subspace tracking algorithms as shown in Section IV. The Taylor series approximation adopted in [5], [30], and [32] can be invoked to obtain the optimal diagonal loading term ε as follows:

$$\begin{aligned}\hat{\boldsymbol{f}}_{\max/\min} &= \left(\boldsymbol{I} + \varepsilon\boldsymbol{R}_{xx}^{-1}\right)^{-1}\boldsymbol{R}_{xx}^{-1}\boldsymbol{C}_1\boldsymbol{g}_{\max/\min}\\ &= \left(\boldsymbol{I} + \varepsilon\boldsymbol{R}_{xx}^{-1}\right)^{-1}\boldsymbol{\Delta}(n)\boldsymbol{g}_{\max/\min}.\end{aligned} \tag{49}$$

Then, using Taylor series approximation, we get

$$\hat{\boldsymbol{f}}_{\max/\min} \approx \left(\boldsymbol{I} - \varepsilon\boldsymbol{R}_{xx}^{-1}\right)\boldsymbol{f}_{\max/\min}. \tag{50}$$

Thus

$$\hat{\boldsymbol{f}}_{\max/\min} \approx \boldsymbol{f}_{\max/\min} - \varepsilon\tilde{\boldsymbol{f}}_{\max/\min} \tag{51}$$

where

$$\tilde{\boldsymbol{f}}_{\max/\min} = \boldsymbol{R}_{xx}^{-1}\boldsymbol{f}_{\max/\min}. \tag{52}$$

Therefore, utilizing the approximation in (51) in the quadratic constraint in (47), the diagonal loading term ε is obtained using a simple quadratic equation with a variable loading technique as in [5]. It is interesting to highlight the drawback of the Taylor series approximation in (51). Specifically, the diagonal loading term ε cannot be precisely calculated owing to this approximation, and even real diagonal loading cannot be guaranteed [5]. Nevertheless, merging the max/min channel estimation technique with the QIC technique produces an optimal MOE detector with robustness against noise enhancement at low SNR [30]. Although this quadratic constraint was proposed in [5], no direct form implementation was provided, and even the proposed direct implementation in [5] is not suitable for channel tracking due to the fact that the matrix inverse update is a projection version of the inverse of the data covariance matrix. The adaptive implementation of this detector using the IQRD-RLS algorithm is appended in Table I. The total multiplications complexity of this detector is about $O(3N_fN_g+2N_g^2+2N_f^2+4N_g+9N_f)$, as shown in Table I.

VI. Systolic Array Implementation of Optimal MOE Receiver

Systolic array implementation of the IQRD-based algorithms is one of the most important merits which would be very beneficial in real-time application and parallel processing. An advantage of the systolic array over other architectures is that the individual processing element computational complexity does not grow with increasing the number of constraints N_g [8]. The IQRD update method is selected for this purpose because the direct QR method requires back-substitution for updating the detector, and hence two opposite direction operations (i.e., triangular update and back substitution) must be concurrently performed [11], [15]. Unfortunately, these two steps cannot be implemented in parallel fashion on triangular arrays and, therefore, one of the most important merits of such methods will be lost.

The optimal MOE detector with the max/min approach implemented using the Lagrange method can be implemented

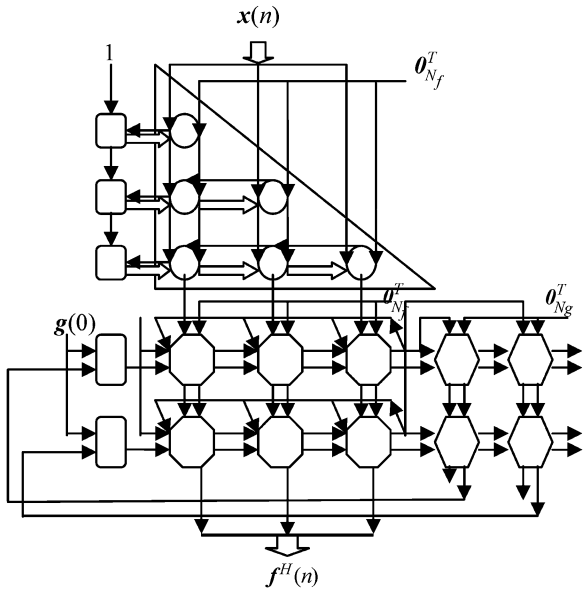

Fig. 1. Systolic array implementation of MOE-IQRD with max/min.

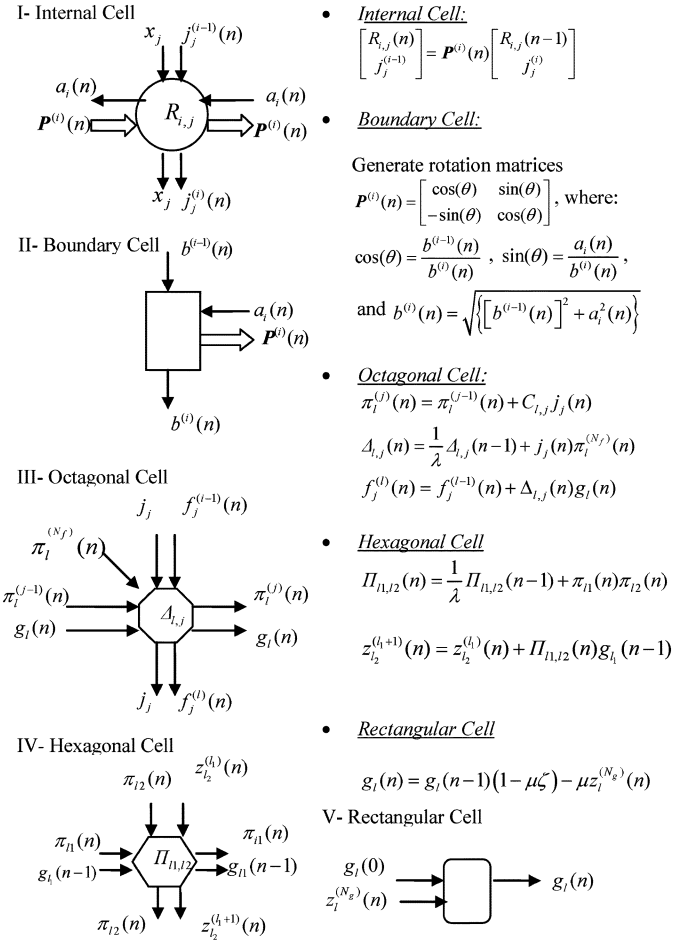

Fig. 2. Definitions of cells used in the systolic array implementation.

using systolic arrays as shown in Fig. 1. The cells exercised in this implementation are the five types of cells as shown in Fig. 2. The internal cells are used to update the inverse Cholesky factor $\boldsymbol{R}^{-H}(n)$, and each cell contains the corresponding $R_{i,j}$, where $i = 1 : N_f$ and $j = 1 : N_f$ and concurrently generates the intermediate vector $\boldsymbol{a}(n)$. The boundary cells use $\boldsymbol{a}(n)$ and $b(n)$ to generate 2×2 rotation matrices $\boldsymbol{P}^{(i)}(n)|_{i=1:N_f}$ as depicted in Fig. 2. The rotation matrix $\boldsymbol{P}(n)$ in (14) can be constructed from $\boldsymbol{P}^{(i)}(n)|_{i=1:N_f}$ [11]. The rotation matrices are exploited in the internal cells to update the inverse *Cholesky* factor $\boldsymbol{R}^{-H}(n)$ as shown in Fig. 2. Therefore, the IQRD systolic implementation is used to update $\boldsymbol{R}^{-H}(n)$ and to generate the $\boldsymbol{j}(n)$ vector using Givens rotations.

The octagonal cell grid with dimension $N_g \times N_f$ is used to update the matrix $\boldsymbol{\Delta}(n)$ and to generate the vector $\boldsymbol{\pi}(n)$ from the last column in the grid, where each cell contains the corresponding $C_{l,j}$ and $\Delta_{l,j}$ where $l = 1 : N_g$. The vector $\boldsymbol{\pi}(n)$ is used to update the matrix $\boldsymbol{\Delta}(n)$ in the octagonal grid and to update the matrix $\boldsymbol{\Pi}(n)$ into a hexagonal cell grid with dimension $N_g \times N_g$. These two steps can be performed concurrently. Each cell in the hexagonal grid contains the corresponding $\boldsymbol{\Pi}_{l1,l2}(n)$, where $l_1 = 1 : N_g$, $l_2 = 1 : N_g$. After update of the matrix $\boldsymbol{\Pi}(n)$, the hexagonal grid generates the matrix multiplication $\boldsymbol{\Pi}(n)\boldsymbol{g}(n-1)$ which feeds the rectangular cells to generate the channel vector $\boldsymbol{g}(n)$. The optimal weight vector can be obtained after the update of $\boldsymbol{\Delta}(n)$ from the last row in the octagonal cell grid. The forthcoming update of channel vector $\boldsymbol{g}(n+1)$ and the vector $\boldsymbol{\pi}(n+1)$ can be done alongside the estimate of the detector $\boldsymbol{f}(n)$.

Note that the computation of the step-size $\mu_{\text{opt}}(n)$ and the diagonal loading term ζ are avoided to facilitate the systolic implementation. The variable step-size can be replaced by a properly selected fixed step-size, and the parameter ζ can be chosen to guarantee that the channel vector is normalized. The definitions of the five cells used in the systolic implementation are described in Fig. 2. In addition, recursive implementations of the processing cells in adaptive fashions are formulated in Fig. 2. Moreover, the recursive systolic algorithm without Kalman gain estimation (i.e., $\boldsymbol{j}(n)$) is formulated in Table II. The complete systolic algorithm can be obtained by appending the algorithm in Table II to the original IQRD-RLS algorithm in [11], which was implemented using Givens rotations.

VII. Examples and Computer Simulations

We consider a CDMA system with five users in a multipath Rayleigh fading channel. Each user's signal scattered in different five multipath components. Orthogonal Gold codes are employed as the signature waveforms and the channel length (max delay spread) is assumed to be ten delayed components, and the multipath delays are randomly distributed. The code length equals 31 chips, and the detector is assumed to span one bit length and is synchronized to the desired user. The desired user has an SNR of 15 dB. The SNR of the interfering users are 10 dB higher than the desired user to model a severe near–far environment. The output SINR and BER are adopted as the performance measures.

A. Experiment 1

In this experiment, the optimal MOE detector with the max/min approach is tested with three subspace tracking algorithms. The first algorithm is the Lagrange method introduced in Section IV and is exploited to track both the MC and the

TABLE II
RECURSIVE SYSTOLIC IMPLEMENTATION OF AN OPTIMAL MOE RECEIVER

- For $l = 1 : N_g$; Octagonal grid row span
  - $\pi_l^{(0)}(n) = 0$
  - For $j = 1 : N_f$; Octagonal grid column span
    - $\pi_l^{(j)}(n) = \pi_l^{(j-1)}(n) + C_{l,j} j_j(n)$
  - End for
  - For $j = 1 : N_f$; Octagonal grid column span
    - $\Delta_{l,j}(n) = \frac{1}{\lambda}\Delta_{l,j}(n-1) + j_j(n)\pi_l^{(N_f)}(n)$; *update of matrix* $\boldsymbol{\Delta}(n)$
  - End for
- End for
- For $l_2 = 1 : N_g$; *Hexagonal grid column span*
  - $z_{l_2}^{(0)}(n) = 0$
  - For $l_1 = 1 : N_g$; *Hexagonal grid row span*
    - $\Pi_{l1,l2}(n) = \frac{1}{\lambda}\Pi_{l1,l2}(n-1) + \pi_{l1}(n)\pi_{l2}(n)$; *update of matrix* $\boldsymbol{\Pi}(n)$
    - $z_{l_2}^{(l_1+1)}(n) = z_{l_2}^{(l_1)}(n) + \Pi_{l1,l2}(n) g_{l_1}(n-1)$; *gradient vector update*
  - End for
- End for
- For $l = 1 : N_g$
  - $g_l(n) = g_l(n-1)\left(1 - \mu\zeta\right) - \mu z_l^{(N_g)}(n)$; *channel vector update*
- End for
- For $j = 1 : N_f$
  - $f_j^{(0)}(n) = 0$
  - For $l = 1 : N_g$
    - $f_j^{(l)}(n) = f_j^{(l-1)}(n) + \Delta_{l,j}(n) g_l(n)$; *final vector computation*
  - End for
- End for

TABLE III
INITIALIZATION PARAMETERS OF SUBSPACE TRACKING ALGORITHMS

Parameter/Method	Lagrange		NOOja	OPASTd
	MC	PC		
σ	0.95	0.001	0.008	N/A
η	0.4	0.4	0.4	N/A
Forgetting factor	N/A	N/A	N/A	0.995

PC. The corresponding MOE detectors are referred to, respectively, as MOE-IQRD w. Lagrange (MC) and MOE-IQRD w. Lagrange (PC). The second algorithm is the NOOja algorithm, which is exploited to track the PC [referred to as MOE-IQRD w. NOOja (PC)]. The third algorithm is the OPASTd algorithm which is employed to track the principal component [referred to as MOE-IQRD w. OPASTd (PC)]. All subspace tracking algorithms are initialized with a normalized channel vector (i.e., $\boldsymbol{g} = [\nu \cdots \nu]^T / ||\boldsymbol{g}||$, where $\nu = 1/N_g$)). Other parameters are summarized in Table III. These parameters are obtained empirically using several numerical simulations.

Figs. 3 and 4 show, respectively, the SINR and BER for the four MOE detectors in addition to a benchmark MOE detector with the actual channel vector (referred to as MOE-IQRD w. Optimal channel). The figures show the superiority of the Lagrange method when used to track the MC. The NOOja algorithm comes in the second grade and then the Lagrange method when used to track the PC. The OPASTd algorithm exhibits the worst performance in terms of the convergence speed. This is because the forgetting factor is set to a relatively small value (0.995). On the other hand, increasing the forgetting factor engenders a faster convergence speed detector at the expense of steady-state performance. It is concluded that the OPASTd algorithm performance can be improved in terms of steady state and convergence speed if a variable forgetting factor technique is adopted to adjust the forgetting factor to an appropriate value during the update process. However, it is noteworthy that the OPASTd algorithm with maximum effort cannot outperform any other subspace tracking algorithm.

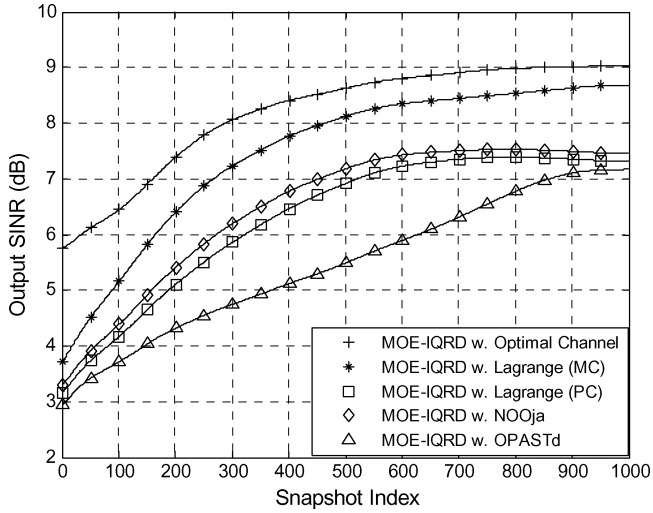

Fig. 3. SINR of the MOE detector with different subspace tracking algorithms

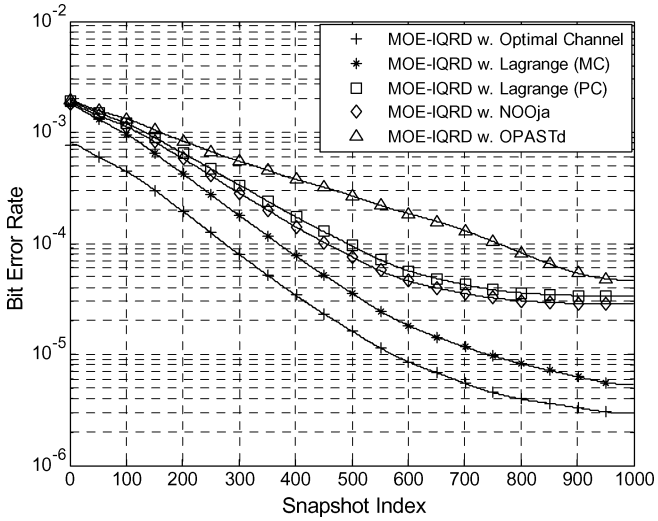

Fig. 4. BER of the MOE detector with different subspace tracking algorithms.

B. Experiment 2

As shown in Section V, several approaches have been developed to overcome noise enhancement associated with an optimal max/min MOE detector. It is interesting to evaluate the robustness of these detectors at low SNR. Therefore, the above system

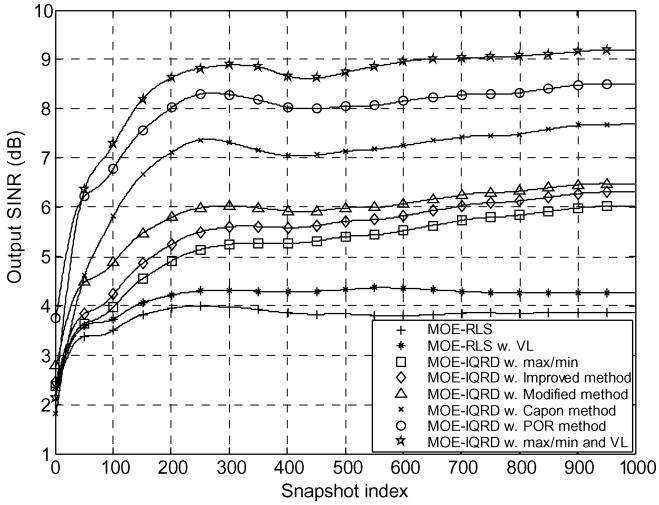

Fig. 5. SINR versus snapshot for different MOE detectors at low SNR.

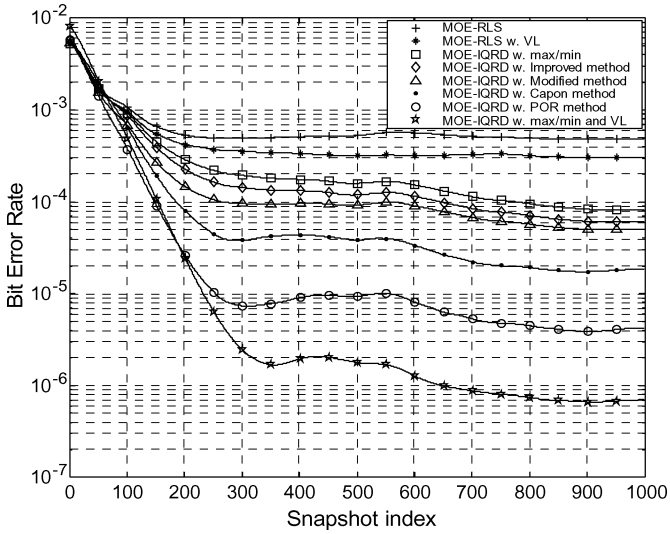

Fig. 6. BER versus snapshot for different MOE detectors at low SNR.

is exercised when the desired user SNR is reduced to 10 dB. In addition, the system experiences an acute near–far effect in a loaded multipath environment with large delay spread. Eight MOE detectors are analyzed in this experiment. The first detector is the MOE detector with an equal-gain channel vector and adapted using the RLS algorithm (referred to as MOE-RLS). The second detector is the MOE-RLS detector with a QIC and a VL technique proposed in [5] (referred to as MOE-RSL w. VL). The third detector is the MOE-IQRD algorithm with the max/min approach (referred to as MOE-IQRD w. max/min method). The fourth detector is the MOE-IQRD algorithm with the improved cost function proposed in [7] (referred to as MOE-IQRD w. improved cost function). The fifth detector is the MOE-IQRD algorithm with the modified cost function proposed in [8] (referred to as MOE-IQRD w. modified cost function). The sixth detector is the POR receiver proposed in [9] (referred to as MOE-IQRD w. POR method). The Capon detector, proposed in [2] and [3], is the seventh detector (referred to as MOE-IQRD w. Capon method). The last detector is the combined max/min and VL technique (referred to as MOE-IQRD w. max/min and VL) which is summarized in Table I. The Lagrange method with MC tracking is employed for tracking the channel vector of the third, fourth, fifth, and eighth detectors. The generalized subspace tracking algorithm proposed in [33] is exploited to track the channel vector of the Capon method which requires the principle generalized eigenvector. All of the detectors, except the first and second, are adapted using the IQRD-based implementations provided in Section V.

Figs. 5 and 6 illustrate, respectively, the SINR and BER for the aforementioned detectors. It is apparent from the figures that the robust approach proposed in [5] offers little improvement over the MOE-RLS detector with an equal-gain channel. The performance of MOE-IQRD w. max/min detector compared with the first experiment is degraded due to decreasing interested user power. A little improvement over MOE-IQRD w. max/min detector is introduced by the MOE-IQRD w. improved cost function detector. The MOE-IQRD w. modified cost function detector introduces additional improvement over the MOE-IQRD w. improved cost function detector. The constant τ of the modified cost function in (42) is adjusted such as $\tau\sigma_w^2 = \sigma_w^2 + 0.5$. If the constant τ is adjusted such as $0 \leq \tau < 1$ as in [8], the performance of MOE-IQRD w. modified cost function detector performs almost similarly to the MOE-IQRD w. max/min detector [21]. This is due to the imperfect estimation of the noise power due to covariance matrix estimation errors. It is noteworthy to highlight that this selection is based on system parameters, noise power, and simulation environment. However, we should be careful to avoid violation of data covariance matrix positiveness. The Capon method comes in the subsequent position with significant improvement and then the POR receiver with additional improvement. The MOE-IQRD w. max/min and VL detector exhibits superior performance over all approaches in terms of SINR and BER.

C. Complexity Analysis

In order to augment the assessment of the MOE detectors exercised in the above experiment, we should compare their complexities. Table IV assesses the above eight MOE detectors in terms of multiplication complexity. The *Cholesky* factor $\boldsymbol{j}(n)$ requires $6N_f$ multiplications [10], [24]. The weight vectors of the MOE-IQRD detectors require $N_f N_g$ multiplications due to the matrix-vector multiplication (i.e., $\boldsymbol{\Delta}(n)\boldsymbol{g}(n)$). Other complexities are summarized in the table. The last column of Table IV summarizes the multiplication complexities for the simulation scenario $(N_f = 31, N_g = 10)$. It is evident from this column that the MOE-IQRD w. max/min detector requires less computational complexity than the MOE-RLS and MOE-RLS w. VL detectors. Nevertheless, it surpasses them in terms of SINR and BER. The MOE-IQRD w. max/min and the MOE-IQRD w. improved cost function detectors require the same complexity. The MOE-IQRD w. modified Cost function detector requires very high computational complexity while it provides slight improvement over the MOE-IQRD w. improved cost function detector. The MOE-IQRD w. max/min and VL detector necessitates less computational complexity than the POR receiver does while it produces a preeminent performance in terms of SINR and BER. Astonishingly, the Capon method requires less computational complexity than the MOE-IQRD w. max/min and VL detector while unfortunately it does not attain

TABLE IV
MULTIPLICATIONS COMPLEXITY COMPARISON AMONG MOE DETECTORS OF EXPERIMENT 2

Detector	Kalman gain	Intermediate matrix update	Channel vector /VL technique	Weight vector	Total complexity	Special case
MOE-RLS	$N_a^2+N_a$	$N_a^2+2N_a+N_fN_a$	-	-	$2N_a^2+3N_a+N_fN_a$	1596
MOE-RLS w. VL	$N_a^2+N_a$	$N_a^2+2N_a+N_fN_a$	$N_a^2+2N_a$ (VL)	-	$3N_a^2+5N_a+N_fN_a$	2079
MOE-IQRD w. max/min	$6N_f$	$2N_fN_g+N_g^2$	$N_g^2+4N_g$ (CH)	N_fN_g	$3N_fN_g+2N_g^2$ $+4N_g+6N_f$	1356
MOE-IQRD w. improved Cost function	$6N_f$	$2N_fN_g+N_g^2$	$N_g^2+4N_g$ (CH)	N_fN_g	$3N_fN_g+2N_g^2$ $+4N_g+6N_f$	1356
MOE-IQRD w. modified Cost function	$6N_f$	$N_fN_g^2+N_f^2$ $+2N_fN_g$	$N_g^2+4N_g$ (CH)	N_fN_g	$N_fN_g^2+N_f^2+3N_fN_g$ $+N_g^2+4N_g+6N_f$	4356
MOE-IQRD w. POR method	$6N_f$	$N_fN_g^2+N_fN_g$	$N_g^2+4N_g$ (CH)	N_fN_g	$N_fN_g^2+2N_fN_g$ $+N_g^2+4N_g+6N_f$	4046
MOE-IQRD w. Capon method	$6N_f$	$2N_g^2+2N_g$ $+2N_fN_g$	$N_g^3+2N_g^2$ (CH) $+2N_g$	N_fN_g	$N_g^3+3N_fN_g+4N_g^2$ $+4N_g+6N_f$	2556
MOE-IQRD w. max/min and VL	$6N_f$	$2N_fN_g+N_g^2$	$N_g^2+4N_g$ (CH) $2N_f^2+3N_f$ (VL)	N_fN_g	$3N_fN_g+2N_g^2+2N_f^2$ $+4N_g+9N_f$	3371

CH and VL stand, respectively, for channel estimation and VL technique complexities, $N_a=N_f-N_g$ and for special case $N_f=31$, $N_g=10$.

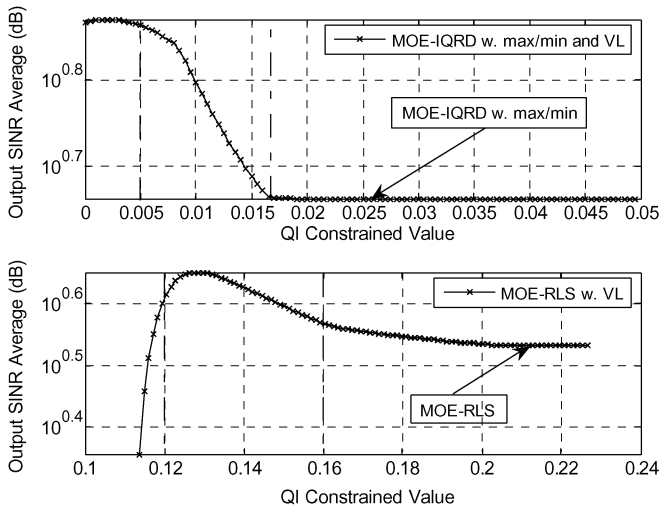

Fig. 7. Effect of ρ on output SINR average of MOE-IQRD w. max/min and VL detector and MOE-RLS w. VL detector.

a similar performance. In addition, the MOE-IQRD w. max/min and VL detector does not execute the VL technique through all recursive steps. Therefore, its computational complexity should be averaged over the number of VL subroutine execution.

D. Experiment 3

Finally, it is significant to compare the MOE-IQRD w. max/min and VL and MOE-RLS w. VL in the context of the QIC effect. The two detectors incorporate a QIC on the weight vector norm while the first does not optimize the channel vector. In order to compare the two detectors, the average output SINR of the interested user is marked against the constrained value (i.e., ρ). Fig. 7 demonstrates the average output SINR of the two detectors versus constrained value. The difference between the maximum attained values by the two detectors is due to channel vector estimation with the first detector. By inspecting this figure, the following observations can be noticed. The MOE-RLS w. VL detector has a key constrained value which engenders the optimal performance of this detector. Unfortunately, there is no closed-form solution for this optimum constrained value. Alternatively, it could be selected based on some preliminary (coarse) knowledge about wireless channels or using Monte Carlo simulation. In contrast, the MOE-IQRD w. max/min and VL detector has an optimum window of constrained values (i.e., $\rho=(0,0.005]$). Therefore, the optimal performance of this detector can be easily obtained. It is important to highlight that the upper bound of the optimum window is not a predetermined value, but it is also scenario-dependent; however, an optimum value can be obtained easily due to the availability of an optimum window.

A further clarification is that the QIC effect on the MOE-RLS w. VL detector can be divided into three regions, as shown in Fig. 7. The central region specifies the optimum region where the VL technique has a graceful effect on the detector performance with optimum constrained value. In the third region, the VL technique no longer affects the algorithm behavior, and hence the detector performance boiled down to the MOE-RLS detector without the QIC. In the first region, the VL technique has an ugly effect on the detector, and its performance is catastrophically degraded in this region. In contrast, the performance of the MOE-IQRD w. max/min and VL detector can be divided into three regions. The first region is the steady-state region with rigid optimality. In the second region, the performance of the detector decreases monotonically with the increase of the constrained value until the effect of the QIC is neglected and the detector converges to the MOE-IQRD w. max/min detector. As a final conclusion, the max/min channel estimation has not only increased the maximum attainable value by the detector but also improved the performance of VL technique.

VIII. Discussion and Conclusion

In this paper, the IORD-RLS algorithm using Givens rotations is exploited to develop numerically robust multiuser detection receivers. The IQRD method is the promising one for this purpose due to pipeline implementation on VLSI, good numerical stability, and no back-substitution. It can also be mapped onto CORDIC processor-based systolic arrays. In this paper, the optimal MOE receiver based on the max/min approach has been implemented using the IQRD-RLS algorithm. A new fast subspace tracking algorithm based on the Lagrange method and the IQRD algorithm has been developed and compared with the recently proposed NOOja and OPASTd subspace tracking algorithms. We verified from computer simulations that the new proposed method is the best in terms of SINR and BER. The OPASTd algorithm exhibits the worst performance, and a variable forgetting factor technique is suggested to improve its performance. In order to overcome noise enhancement associated with the max/min approach, a robust detector anchored in the optimal MOE-IQRD w. max/min detector along with a QIC on the weight vector is proposed. Other recently introduced robust MOE receivers have been summarized and implemented using the IQRD-RLS algorithm. The MOE-IQRD w. max/min and VL detector is shown to outperform the recently proposed robust detectors in terms of SINR and BER at low SNR in a loaded multipath system with severe near–far effect. Furthermore, it requires moderate computational load compared with other approaches. The possibility of systolic array implementation of the optimal MOE-IQRD w. max/min detector is analyzed. A new systolic implementation of the optimal max/min MOE detector with the proposed subspace tracking algorithm is proposed. Future research may include studying the hardware implementation problems to these algorithms. Also, other fast QRD-RLS algorithms, which are computationally more efficient like square-root free algorithms and scaled version of fast Givens rotations may be developed and adopted for MUD applications.

References

[1] M. K. Tsatsanis, "Inverse filtering criteria for CDMA systems," *IEEE Trans. Signal Process.*, vol. 45, no. 1, pp. 102–112, Jan. 1997.

[2] M. K. Tsatsanis and Z. Xu, "On minimum output energy CDMA receives in presence of multipath," in *Proc. Conf. Inf. Sci. Syst.*, 1997, pp. 377–381.

[3] M. K. Tsatsanis and Z. Xu, "Performance analysis of minimum variance CDMA receivers," *IEEE Trans. Signal Process.*, vol. 46, no. 11, pp. 3014–3022, Nov. 1998.

[4] Z. Xu and M. K. Tsatsanis, "Blind adaptive algorithms for minimum variance CDMA receivers," *IEEE Trans. Signal Process.*, vol. 49, no. 1, pp. 180–194, Jan. 2001.

[5] Z. Tian, K. L. Bell, and H. L. Van Trees, "Robust constrained linear receivers for CDMA wireless systems," *IEEE Trans. Signal Process.*, vol. 49, no. 7, pp. 1510–1522, Jul. 2001.

[6] A. Elnashar, S. Elnoubi, and H. Elmikati, "A robust quadratically constrained adaptive blind multiuser detection for DS/CDMA systems," in *Proc. ISSSTA2004*, Sydney, Australia, 2004, pp. 164–168.

[7] Z. Xu, "Improved constraint for multipath mitigation in constrained MOE multiuser detection," *J. Commun. Netw.*, vol. 3, no. 3, pp. 189–198, Sep. 2002.

[8] Z. Xu, "Further study on MOE-based multiuser detection in unknown multipath," *EURASIP J. Appl. Signal Process.: Multiuser Detection Blind Estim.*, pp. 1377–1386, Dec. 2002.

[9] Z. Xu, P. Liu, and X. Wang, "Blind multiuser detection: From MOE to subspace methods," *IEEE Trans. Signal Process.*, vol. 52, no. 2, pp. 510–524, Feb. 2004.

[10] S.-J. Chern and C.-Y. Chang, "Adaptive linearly constrained inverse QRD-RLS beamforming algorithm for moving jammers suppression," *IEEE Trans. Antennas Propag.*, vol. 50, no. 8, pp. 1138–1150, Aug. 2002.

[11] S. T. Alexander and A. L. Ghirnikar, "A method for recursive least squares filtering based upon an inverse QR decomposition," *IEEE Trans. Signal Process.*, vol. 41, no. 1, pp. 20–30, Jan. 1993.

[12] H. V. Poor and X. Wang, "Code-aided interference suppression for DS/CDMA communications—Part II: Parallel blind adaptive implementations," *IEEE Trans. Commun.*, vol. 45, no. 9, pp. 1112–1122, Sep. 1997.

[13] L. Gao and K. Parhi, "Hierarchical pipelining and folding of QRD-RLS adaptive filtering and its application to digital beamforming," *IEEE Trans. Circuits Syst. I, Fundam. Theory Appl.*, vol. 47, no. 12, pp. 1503–1519, Dec. 2000.

[14] M. Moonen and I. K. Roudler, "MVDR beamforming and generalized sidelobe cancellation based on inverse updating with residual extraction," *IEEE Trans. Circuits Syst. I, Fundam. Theory Appl.*, vol. 47, no. 4, pp. 352–358, Apr. 2000.

[15] J. Ma, K. Parhi, and E. F. Deprettere, "Annihilation-reordering look-Ahead pipelined CORDIC-based RLS adaptive filters and their application to adaptive beamforming," *IEEE Trans. Signal Process.*, vol. 48, no. 8, pp. 2414–2431, Aug. 2000.

[16] A. Elnashar, S. Elnoubi, and H. Elmikati, "A novel adaptive blind multiuser receiver for DS/CDMA based on combined inverse QRD-RLS algorithm and constrained optimization approach," in *Proc. Int. Symp. Intell. Signal Process. Commun. Syst. Conf.*, 2003, pp. 423–428.

[17] A. Elnashar, S. Elnoubi, and H. Elmikati, "A robust adaptive blind multiuser detection for DS/CDMA based on combined inverse QRD-RLS algorithm and MOE," in *Proc. SOFTCOM Conf.*, 2003, pp. 512–515.

[18] A. Elnashar, S. Elnoubi, and H. Elmikati, "Computationally efficient real-time blind multiuser detection for cellular DS/CDMA based on inverse QRD-RLS and subspace tracking," in *Proc. Midwest Symp. Circuits Syst.*, 2003, pp. 303–306.

[19] S.-J. Chern, C.-Y. Chang, and H.-C. Liu, "Multiuser wavelet based MC-CDMA receiver with linearly constrained constant modulus IQRD-RLS algorithm," in *Proc IEEE Int. Symp. Circuits Syst.*, 2002, pp. 193–196.

[20] S.-J. Chern and C.-Y. Chang, "Adaptive MC-CDMA receiver with constrained constant modulus IQRD-RLS algorithm for MAI suppression," *Signal Process.*, vol. 83, pp. 2209–2226, Oct. 2003.

[21] A. Elnashar, S. Elnoubi, and H. Elmikati, "Performance analysis of robust MOE detectors at low SNR based on the IQRD-RLS algorithm," in *Proc. IST Mobile Wireless Commun. Summit*, Myconos, Greece, Jun. 4–8, 2006.

[22] Y. S. Song, H. M. Kwon, and B. J. Min, "Computationally efficient smart antennas for CDMA wireless communications," *IEEE Trans. Veh. Technol.*, vol. 50, no. 6, Nov. 2001.

[23] A. Elnashar, "Multiuser interference cancellation in cellular code division multiple access systems," Ph.D. dissertation, Dept. Electron. and Commun. Eng., Mansoura Univ., Mansoura, Egypt, 2005.

[24] M. Moonen, "Systolic MVDR beamforming with inverse updating," in *Proc. Inst. Elect. Eng.*, 1993, vol. 140, pp. 175–178.

[25] S. F. Hsieh, K. L. R. Liu, and K. Yao, "A unified square-root-free approach for QRD-based recursive least squares estimation," *IEEE Trans. Signal Process.*, vol. 41, no. 3, pp. 1405–1409, Mar. 1993.

[26] S. Haykin, *Adaptive Filter Theory*, 4th ed. Upper Saddle River, NJ: Prentice-Hall, 2002.

[27] K. Abed-Meraim, A. Chkeif, and Y. Hua, "Fast orthogonal PAST algorithm," *IEEE Trans. Signal Process. Lett.*, vol. 7, no. 3, pp. 60–62, Mar. 2000.

[28] S. Attallah and K. Abed-Meraim, "Fast algorithms for subspace tracking," *IEEE Trans. Signal Process. Lett.*, vol. 8, no. 7, pp. 203–206, Jul. 2001.

[29] S. Choi and D. Shim, "A novel adaptive beamforming algorithm for a smart antenna in a CDMA mobile communication environment," *IEEE Trans. Veh. Technol.*, vol. 49, no. 5, pp. 1793–1806, Sep. 2000.

[30] A. Elnashar, S. Elnoubi, and H. Elmikati, "Further study on robust Adaptive beamforming with optimum diagonal loading," *IEEE Trans. Antennas Propag.*, vol. 54, no. 12, pp. 3647–3658, Dec. 2006.

[31] J. Li, P. Stoica, and Z. Wang, "Doubly constrained robust Capon beamformer," *IEEE Trans. Signal Process.*, vol. 52, no. 9, pp. 2407–2423, Sep. 2004.

[32] M. W. Ganz, R. L. Moses, and S. L. Wilson, "Convergence of the SMI and diagonally loaded SMI algorithm with weak interference," *IEEE Trans. Antennas Propag.*, vol. 38, no. 3, Mar. 1990.

[33] Y. N. Rao, J. C. Principe, and T. F. Wong, "Fast RLS-like algorithm for generalized eigendecomposition and its application," *J. VLSI Signal Process.*, vol. 37, no. 2–3, pp. 333–344, Jun.–Jul. 2004.

Ayman Elnashar was born in Egypt in 1972. He received the B.S. degree in electrical engineering from Alexandria University, Alexandria, Egypt, in 1995, and the M.Sc. and Ph.D. degrees in electrical communications engineering from Mansoura University, Mansoura, Egypt, in 1999 and 2005, respectively.

From March 1997 to March 1998, he was an RF Design Engineer with Systel (Motorola Egypt). From March 1998 to February 2000, he was an RF Systems Engineer with the Wireless Laboratory of Egypt Electrical Authority (EEA), Mansoura. From March 2000 to June 2005, he was with the Egyptian Company for Mobile Services (MobiNil), Cairo, Egypt. He was with the Department of Mobile Network Development (MND), Etihad Etisalat (Mobily), Riyadh, Saudi Arabia, from June 2005 to January 2008. He was responsible for radio access network development and implementation. He has been engaged in the design, planning, and implementation of Mobily UMTS network, HSDPA broadband evolution, and the DVB-H pilot network. Currently, he is a Senior Manger, Access Network, in Technology Development Department, Emirates Integrated Telecommunications Company PJSC (du), Dubai, UAE. He is responsible for the access network deployment and implementation. His research interests include digital signal processing for wireless communications, cellular systems, multiuser detection, smart antenna, array processing, beamforming, and robust adaptive detection.

Dr. Elnashar has been a technical reviewer of the IEEE TRANSACTIONS ON VEHICULAR TECHNOLOGY, the IEEE TRANSACTIONS ON SIGNAL PROCESSING, the IEEE TRANSACTIONS ON WIRELESS COMMUNICATIONS, *IET Signal Processing*, and the *EURASIP Journal on Applied Signal Processing*.

Said Elnoubi was born in Alexandria, Egypt, in September 1951. He received the B.S. and M.S. degrees from Alexandria University, Alexandria, in 1974 and 1977, respectively, and the Ph.D. degree from Southern Methodist University, Dallas, TX, in 1980, all in electrical engineering.

From October 1974 to December 1977, he was an Instructor with Alexandria University. From January 1978 to December 1980, he was a Research Assistant with Southern Methodist University and, from January 1981 to August 1981, he was a Postdoctoral Fellow at the same university. From September 1981 to August 1987, he was an Assistant Professor of electrical engineering with the University of Illinois, Chicago, IL. From September 1987 to June 1989, he was an Associate Professor with the Electrical Engineering Department, Alexandria University. From August 1989 to May 1990, he was a Visiting Professor with Wichita State University, Wichita, KS. From 1990 to 1994, he was a member of the Technical Staff with MITRE Corporation, McLean, VA. Currently, he is a Professor and Chairman of the Electrical Engineering Department, Alexandria University. He is a part-time consultant to Sysdsoft, designing wireless communication systems. His research interests include digital modulation, mobile radio and wireless communications, spread spectrum, and air/ground radio communications.

Dr. Elnoubi has been a technical reviewer of the IEEE TRANSACTIONS ON COMMUNICATIONS, the IEEE TRANSACTIONS ON AEROSPACE AND ELECTRONIC SYSTEMS, the IEEE TRANSACTIONS ON VEHICULAR TECHNOLOGY, the IEEE TRANSACTIONS ON INFORMATION THEORY, and *IEE Proceedings*. He was the Assistant Editor of Communications for the IEEE TRANSACTIONS ON VEHICULAR TECHNOLOGY. He was the recipient of the Egypt National Incentive Award for Engineering Science and the Salah Amer Incentive Award for Electronic Science in 1989, as well as the Egypt National Superiority Award for Engineering Science in 2003 and Alexandria University Distinction Award for Engineering Science in 2004. He is listed in *Marquis Who's Who in Science and Engineering*.

Hamdi A. El-Mikati (M'85–SM'96) received the B.Sc. and M.Sc. degrees in electrical engineering from Alexandria University, Alexandria, Egypt, in 1964 and 1969, respectively, and the Ph.D. degree from the Polytechnic Institute, Leningrad, U.S.S.R, in 1974.

Since 1975, he has been with the Faculty of Engineering, Mansoura University, Mansoura, Egypt, where he is currently a Professor of microwave communications. He was Head of the Department of Electronic Engineering from 1989 to 1992, Vice Dean of the Faculty of Engineering from 1994 until 1998, and Dean of the Faculty from 1998 to 2003. His current interests include antenna arrays for wireless communications, microstrip antenna arrays, and computational electromagnetics.

Dr. El-Mikati is a member of the Optical Society of America and the National Radio Science Committee.